QUANTUM BEATS AND CLASSICAL ORBITS IN MEAN-FIELD SYSTEMS

M. BRACK
Institut für Theoretische Physik, Universität Regensburg
D-93040 Regensburg, Germany

ABSTRACT

The single-particle level density of a mean-field system usually oscillates around its smooth part. The oscillating part can be accounted for in terms of classical periodic orbits. A particularly nice manifestation of this connection between quantum-mechanics and classical orbits is the occurrence of quantum beats in the level density, when only two or a few periodic orbits dominate. After a brief review of the periodic orbit theory developed by Balian and Bloch and by Gutzwiller, we discuss two examples of mean-field systems which exhibit quantum beats: 1. large spherical alkali metal clusters where the interference of triangular and square classical electronic orbits lead to experimentally observable "supershells"; 2. the two-dimensional anharmonic potential of Hénon and Heiles where the classical motion becomes chaotic at higher energies and where the three shortest periodic orbits lead to a beating density of eigenstates.

1. Periodic orbit theory

Let us assume that we know the energy levels ε_n of a system, given by its Hamiltonian $\hat{H}$ through the Schrödinger equation $\hat{H}\varphi_n(\mathbf{r}) = \varepsilon_n\varphi_n(\mathbf{r})$. The level density of this system is defined as the sum of delta functions:

$$g(E) = \sum_n \delta(E - \varepsilon_n), \tag{1}$$

where n runs over the complete spectrum including degeneracies. It has been recognized that $g(E)$ always can be written as a sum of an average part $\tilde{g}(E)$ and an oscillating part $\delta g(E)$:

$$g(E) = \tilde{g}(E) + \delta g(E). \tag{2}$$

The average part is given by the extended Thomas-Fermi model[1] through a phase space average. It may also be numerically obtained from the spectrum $\{\varepsilon_n\}$ by means of the Strutinsky averaging method.[2] Both methods have been shown to agree analytically for the harmonic oscillator and within acceptable numerical accuracy for realistic nuclear potentials.[3]

Presently we shall be concerned with the oscillating part $\delta g(E)$ of the level density. Gutzwiller[4] and Balian and Bloch[5] have independently derived semiclassical approximations to $\delta g(E)$ in terms of the *periodic orbits* of the *classical* system, given as

solutions of the equations of motion derived from the corresponding classical Hamiltonian H_{cl}. These approaches have later been modified and extended by many authors to what is now generally called the "periodic orbit theory" (POT). Common to these approaches is the resulting general form of $\delta g(E)$ which Gutzwiller termed the "trace formula":

$$\delta g\,(E) = \sum_{\lambda} \sum_{k=1}^{\infty} \mathcal{A}_{\lambda k}(E) \cos\left[k\left(\frac{1}{\hbar} S_{\lambda}(E) - \sigma_{\lambda}\frac{\pi}{2}\right)\right]. \tag{3}$$

Here λ goes over all primitive periodic orbits; k counts the number of revolutions around each primitive orbit, yielding a series of harmonics; $S_{\lambda}(E)=\oint \mathbf{p}_{\lambda} \cdot d\mathbf{q}_{\lambda}$ is the classical action integral along the primitive orbit λ; and the Maslov index σ_{λ} is a phase depending on its topology. The amplitude $\mathcal{A}_{\lambda k}$ depends on the energy, the time period $T_{\lambda}=dS_{\lambda}/dE$ and the stability of the orbit; the way to calculate it depends on the orbit being isolated or non-isolated. The latter case occurs in systems with symmetries; then the non-isolated orbits are degenerate with respect to some parameter(s) and λ counts entire families of such degenerate orbits.

Let us illustrate the structure of the decomposition (2) for a very simple example. For a two-dimensional isotropic harmonic oscillator with frequency ω, the total exact level density can be given analytically as:

$$g(E) = \frac{E}{(\hbar\omega)^2}\left\{1 + 2\sum_{k=1}^{\infty} \cos\left(2\pi k \frac{E}{\hbar\omega}\right)\right\}. \tag{4}$$

The first term in Eq. (4) is the smooth part and identical to the Thomas-Fermi expression. The oscillating part consist of one single harmonic series, since there is only one family of degenerate classical orbits (namely ellipses or circles) with identical actions $S=2\pi E/\omega$, amplitudes $2E/(\hbar\omega)^2$ and Maslov indices which fall out. [Note that Gutzwiller's expression for the amplitudes does not apply here due to the degeneracy of the harmonic-oscillator orbits. The easiest way to derive Eq. (4) is to Laplace invert the analytically known partition function using the residue theorem.[6,7]]

The most ambitious goal of the POT is the full quantisation of the system, i.e., to find the spectrum $\{\varepsilon_n\}$ from the singularities of $\delta g(E)$. This goal is, however, very difficult to reach since the sum over periodic orbits in Eq. (3) is asymptotic in nature and often does not converge. The most spectacular results have been obtained with Gutzwiller's trace formula in systems that exhibit classical chaos. We refer to the book of Gutzwiller[8] for an exhaustive discussion of the POT and many applications. (For some newer developments, see also the proceedings of a recent workshop on periodic orbit theory.[9])

We shall discuss here an application of the POT which is much less ambitious and aims at the semiclassical calculation of the *gross-shell structure* in mean-field systems. Noticing that Eq. (3) essentially consists of a Fourier decomposition of the oscillating level density, it is obvious that all higher harmonics with $k > 1$ and all periodic orbits with large actions (which are usually those with large periods and lengths) only determine the finer details of the level density. The gross features of the shell effects in $g(E)$ do not depend on these details and should only be given by the lowest harmonics of the shortest periodic orbits. This was actually the main motivation of the work of Balian and Bloch,[5] and we shall come back to their work in the next section. Strutinsky and collaborators[10] used this approach successfully to explain the nuclear ground-state

deformations as functions of nucleon number A for realistic Woods-Saxon and Nilsson potentials.

In order to study the gross-shell structure starting from a quantum-mechanical spectrum $\{\varepsilon_n\}$, it is useful to *coarse-grain* the exact level density (1) by averaging it over an energy interval of about half the fundamental energy period $\hbar\Omega$ of its oscillating part, corresponding to the main shell spacing in the spectrum ($\hbar\omega$ for a harmonic oscillator). In this way, the higher harmonics and contributions from longer classical orbits are automatically filtered out. Subtracting from it the numerically averaged part $\tilde{g}(E)$ yields a quantum-mechanically determined $\delta g(E)$ which still contains the most important shell effects but is more easily interpreted in terms of classical periodic orbits than the full oscillating level density including the delta function singularities. It is exactly this coarse-grained quantity $\delta g(E)$ which serves as a starting ingredient to Strutinsky's shell-correction method,[2] well-known to nuclear physicists.

A particularly nice manifestation of the role of classical orbits is their possible interference: if two or a few orbits have comparable amplitudes and actions, the superposition of their contributions to Eq. (3) leads to a *beating* amplitude of the level density. As a simple illustration of such a quantum beat, we show in Fig. 1 the oscillating level density of a slightly anisotropic two-dimensional harmonic oscillator with frequency ratio 16:15. The $\delta g(E)$ in Fig. 1 was obtained from the exact quantum spectrum by the coarse-graining method just mentioned.

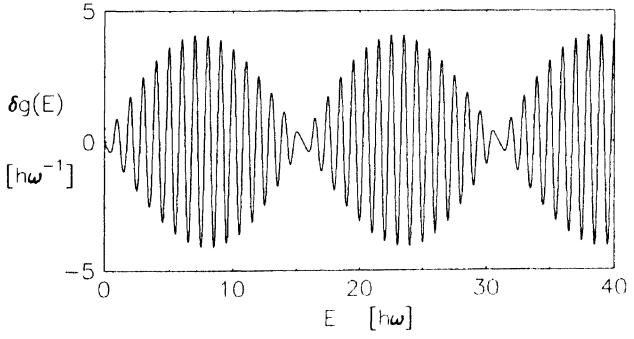

Fig. 1: Oscillating part of the level density of a 2-dimensional harmonic oscillator with frequency ratio 16:15

The analytical $g(E)$ in Eq. (4) above can easily be generalized to the anisotropic case. For *rational* frequency ratios, the result looks rather complicated, but is actually not required here. Indeed, since it is always possible to choose an irrational number which is infinitesimally close to any given rational number, it is sufficient here to give the result for two *incommensurate* frequencies ω_1 and ω_2, which reads[7]

$$g(E) = \frac{1}{\hbar\omega_1\hbar\omega_2}\,E \;+\; \frac{1}{\hbar\omega_1}\sum_{k=1}^{\infty}(-1)^k\left[\sin\left(k\pi\frac{\omega_2}{\omega_1}\right)\right]^{-1}\sin\left(k\frac{2\pi E}{\hbar\omega_1}\right) + \frac{1}{\hbar\omega_2}\sum_{k=1}^{\infty}(-1)^k\left[\sin\left(k\pi\frac{\omega_1}{\omega_2}\right)\right]^{-1}\sin\left(k\frac{2\pi E}{\hbar\omega_2}\right). \qquad (5)$$

To interpret the numerical result in Fig. 1, we just take the lowest harmonics (k=1) and find after some expansion, indeed, that $\delta g(E) \propto \cos(2\pi E/\hbar\omega)\sin(2\pi E/30\hbar\omega)$ (having normalized the frequencies to $\hbar\omega_1\hbar\omega_2=\hbar\omega^2$, as it was done also in the figure), thus giving the correct beat with a fast oscillation of the fundamental period 1 $\hbar\omega$ and an oscillating amplitude with period 30 $\hbar\omega$ – as the result of an interference between the two shortest classical periodic orbits.

After this almost trivial example, we shall in the following sections discuss two occurrences of quantum beats in mean-field systems: one in a integrable system with assumed spherical symmetry where the Balian-Bloch theory applies, and one in a classically chaotic system with only isolated periodic orbits where the original trace formula of Gutzwiller can be used.

2. Supershells in large alkali metal clusters

Metal clusters have become an interesting object of research, representing finite fermion systems whose sizes reach from microscopic to mesoscopic scales.[11] In particular, clusters consisting of alkali and other simple-metal atoms exhibit electronic shell effects which can be associated with closed spherical shells in the mean-field felt by the valence electrons.[12,13] One rather spectacular aspect of their shell structure is the occurrence of so-called supershells[14,15] which find a nice interpretation in terms of classical periodic orbits in a spherical cavity, as studied by Balian and Bloch[5] over 20 years ago.

Due to space limitations we shall here discuss this topic – which is well covered in the literature – only very briefly and without illustrations. (A recent, more explicit presentation may be found in Sec. V.A of Ref. 16.)

The simplest model to describe metal clusters selfconsistently, especially for large sizes where *ab initio* methods are too time consuming, is the so-called jellium model in which the ionic charge distribution of the clusters is averaged out and replaced by a uniform background density. (See, e.g., Ref. 16 for a recent review article on the jellium model and its applications.) This model explains, indeed, the "magic numbers" N_i of atoms, for which the metal clusters are particularly stable and thus particularly abundant in cluster beam experiments,[11] as the numbers of valence electrons in filled major spherical shells in the selfconsistent mean field. These magic numbers occur – for sufficiently hot clusters which can be assumed to be in a melted phase – with a periodicity that corresponds to equidistant radii $R_i=r_sN_i^{1/3}$ (r_s being the Wigner-Seitz radius), where the experimental increment is $\Delta N_i^{1/3} = 0.61 \pm 0.01$ for $N_i \gtrsim 100$, independently of the nature of the alkali atom (i.e., independently of r_s).

In their pioneering work, Balian and Bloch[5] studied the density of eigenstates in a spherical potential with infinitely steep walls. If its oscillating part is coarse-grained, it exhibits a pronounced beating pattern looking very much like that of Fig. 1 when plotted as a function of $\sqrt{E}$. This beat has been obtained semiclassically by Balian and Bloch as the interference of triangular and quadratic classical orbits. In fact, deriving a formula similar to Eq. (3) from a multiple-reflexion expansion of the Green's function, they showed that the leading contributions to $\delta g(E)$ come from periodic orbits in the form of triangles and squares, whereas the amplitudes of all others (diameter, polygons, stars, etc.) are considerably smaller and are responsible only for the finer details of $\delta g(E)$, in particular around the interference minima.

The mean-fields of the valence electrons obtained in jellium model calculations[12] have a Woods-Saxon type shape with rather steep walls. Nishioka *et al.*[14] therefore expected that similar beats might show up in the level densities of metal clusters. They substantiated their prediction by semiclassical calculations with a Woods-Saxon potential fitted to the jellium-model results of Ekardt[12] and termed the groups of spherical shells separated by the interference minima "supershells". The supershell structure of the level density δg, and of the shell-correction energy δE derived from it,[2] has later been confirmed in selfconsistent jellium calculations with up to $N \sim 3000$ atoms.[17] Experimentally, the supershell beats have been observed directly in the oscillating part of the mass abundances in supersonic cluster beams by Pedersen *et al.*[15] after a careful subtraction of the smooth ionic background and a compensation of the temperature suppression of their amplitude.

In a cavity with reflecting walls, the classical trajectories consist of straight lines with actions proportional to their lengths: $S = Lp = L\sqrt{2mE}$. According to Balian and Bloch, the fast oscillations of the level density δg, as a function of $\sqrt{E}$, inside the supershells should thus have a period given by the *average* length $\bar{L} = 5.42R = 5.42r_s N^{1/3}$ of triangles and squares. Quantizing the action $S = \hbar k_F \bar{L}$ and using the Fermi momentum $k_F = 2\pi/3.27r_s$ of the valence electrons, this leads to an increment of magic numbers $\Delta N_i^{1/3} = 3.27/5.42 = 0.603$ which is independent of r_s and in excellent agreement with experiment. The jellium model also gives the same increment within less than one percent. The beat length is given by the *difference* in the lengths of triangles and squares; it translates to a region $800 \lesssim N \lesssim 1200$ where the beat minimum occurs, again in good agreement with experiment.

3. Quantum beats in the Hénon-Heiles spectrum

The two-dimensional potential by Hénon and Heiles (HH),[18] originally designed to model the mean-field felt by a star in a galaxy, has become a textbook example for a system that exhibits chaos at sufficiently high energy. The potential consists of a harmonic oscillator term and a cubic anharmonic term and is given in polar co-ordinates (r, θ) by

$$V_{HH} = \frac{1}{2}r^2 + \frac{\alpha}{3}r^3 \sin(3\theta). \tag{6}$$

(Following the usual convention, we have put $\hbar$=m=ω=1.) α is a parameter whose strength determines the anharmonicity. The potential V_{HH} has a three-fold symmetry with respect to rotations around 120 and 240 degrees. Fig. 2 shows the equipotential lines. The heavy lines labeled A,B,C indicate the three shortest types of classical periodic orbits discussed further below.

A classical particle can escape from this potential over three barriers if its energy is larger than the threshold energy. Below threshold the motion is confined; it becomes less regular with increasing energy and is fully chaotic near the threshold[18] (cf. also Fig. 3 below). Along the three symmetry axes $\theta = \pi/2$, $(\pi/2+2\pi/3)$, and $(\pi/2+4\pi/3)$, we have $\sin(3\theta) = -1$ so that the barrier height is minimum; the threshold energy there is $E^* = 1/6\alpha^2$ (in units of $\hbar\omega$=1). The contours at the threshold energy $E = E^*$ form three straight lines intersecting at the saddle points and forming an equilateral triangle.

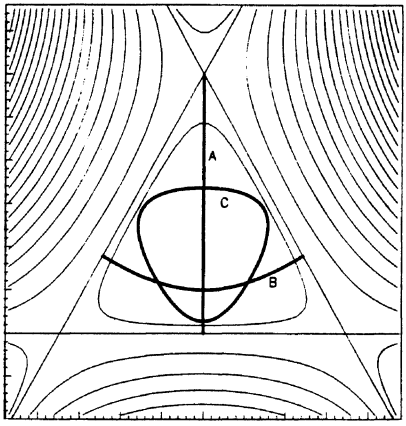

Fig. 2: Contour plot of equipotential lines for the Hénon-Heiles potential
Heavy lines: the three shortest periodic orbits (see text).

It has recently been shown[19] that the quantum level density of the HH potential exhibits a clear beat structure which can be explained in terms of POT. We shall give here a brief outline of this analysis and refer to Refs. 19,20 for the details.

The quantum spectrum ε_n of the potential (6) was obtained by diagonalisation in a large harmonic oscillator basis; barrier tunnelling was neglected, i.e., the states with $\varepsilon_n < E^*$ were taken to have zero imaginary parts. The coarse-grained quantum-mechanical level density $\delta g_{qm}(E)$ is shown in the upper row of Fig. 5 below for three values of α. Only the energy regions $E < E^*$ are displayed. Note the clear beat structure which scales in energy approximately like $1/\alpha$.

In order to interpret this beat structure in terms of classical periodic orbits, we have to solve the equations of motion for the Hamiltonian $H = (p_x^2 + p_y^2)/2 + V_{HH}(x, y)$. This is done most elegantly by scaling away the anharmonicity parameter α, defining the scaled variables $u = \alpha x$ and $v = \alpha y$. The classical equations of motion are then universal in the coordinates u, v, with a dimensionless scaled energy e defined by $e = E/E^* = 6\alpha^2 E$. Having solved the equations of motion for a given e, one can obtain the solutions for all corresponding combinations of E and α.

For a scaled energy $e \lesssim 0.8$, it is well established[19,21] that there are only three types of isolated periodic orbits, shown by the heavy lines in Fig. 2 (for e=1), with periods close to that of the harmonic oscillator, $T_0 = 2\pi/\omega$. They are (A) a one-dimensional oscillation along one of the three symmetry axes, (B) a curved libration ("smiley" orbit) which intersects a symmetry axis at a right angle, and (C) a "loop" orbit which goes around the centre. Due to the symmetry of the HH potential, orbits A and B exist in three distinct versions, whereas C is mapped onto itself under rotations around 120 and 240 degrees. Orbit A is stable up to $e \sim 0.78$; for higher energies $e < 1$ it becomes repeatedly stable and unstable in a periodic fashion;[21] it ceases to exist at $e = 1$ where its period T becomes infinite (however, with finite action S). Orbit C is stable up to $e \sim 0.88$ and unstable at all higher energies. Orbit B is always unstable. Both orbits B and C exist also well above the threshold energy $e = 1$. All other periodic orbits have

periods more than twice T_0 or exist only at higher energies.

In order to exhibit the chaotic nature of the classical motion, we show in Fig. 3 what happens if one observes the orbits B and C at energy e=1 on a computer over many time periods. Since they are unstable, the tiniest numerical noise will let them diverge after a few time periods. This is clearly seen in the upper part of Fig. 3, where the orbits are shown in co-ordinate (u, v) space. Orbit C stays quasi-regular, oscillating between the C-loop shape and a clover-like double-loop orbit which is known to exist at $e \gtrsim 0.88$ and is stable around $e \sim 1$. Orbit B, however, becomes fully chaotic.

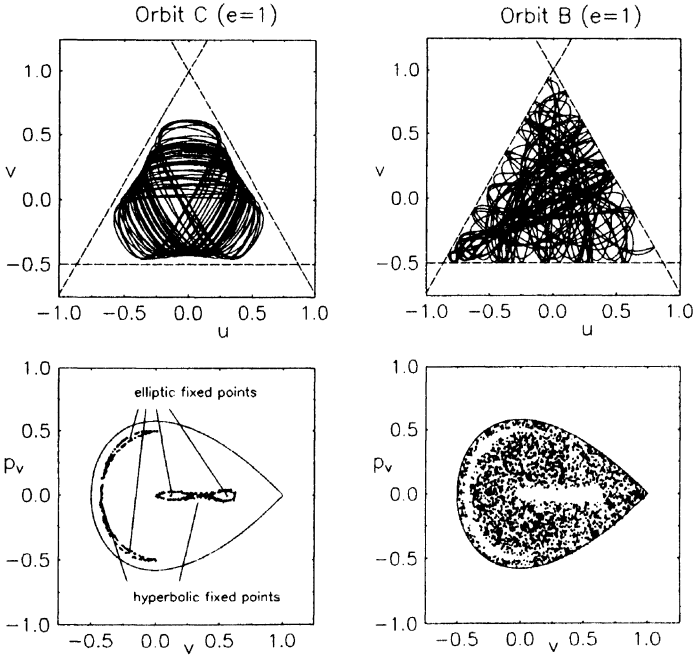

Fig. 3: A quasi-regular orbit (C, left) and a chaotic orbit (B, right) in coordinate (upper part) and phase space (lower part).

The difference between quasi-regular and chaotic motion is most strikingly exhibited phase-space. The surfaces of section, obtained by making a dot in the (p_v, v) plane whenever the particle intersects the u=0 plane (so-called Poincaré sections), are shown in the lower part of Fig. 3. We see that the chaotic orbit derived from B fills almost all the available phase space (given in the p_v, v plane by the drop-like boundary); only a small region is left "blank". This is exactly where the phase-space points of the quasi-regular orbit derived from C fit in. (The hyperbolic fixed points indicated in the lower left of Fig. 3 correspond to the unstable orbit C, whereas the elliptic points belong the the stable double-loop orbit which has approximately twice the period of C.) In the quantum spectrum $\{\varepsilon_n\}$, it has been verified that the nearest-neighbour spacings, like for most chaotic systems, exhibit a Wigner-like $P(s)$ distribution.[20]

In Fig. 4 we show the Fourier transform of the quantum level density $\delta g(E)$ (for α=0.04, see the upper left part of Fig. 5 below). The spectrum in the time domain

shows clear signals around the period $2\pi/\omega$ and some small peaks around the double period. The three most pronounced peaks can be identified with the periods of the three orbits A, B and C which are all close to the unperturbed harmonic-oscillator period $T_0 = 2\pi/\omega$ (the structures at the double period just being their first harmonics).

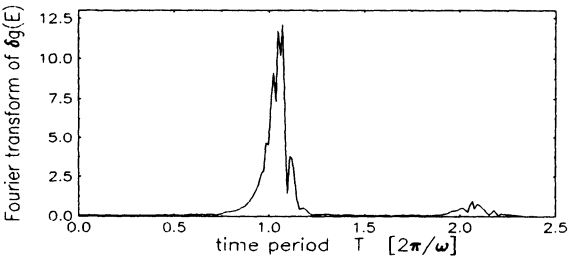

Fig. 4: Fourier transform of $\delta g(E)$ for the HH potential (α=0.04).

Indeed, in the low-energy limit $E \to 0$, the actions $S_\lambda(E)$ of all three orbits go over to that of the harmonic oscillator, $S_0 = 2\pi E/\omega$, and thus the periods go to T_0. However, the energy dependence of $S_\lambda(E)$ is not linear; the numerically calculated scaled actions $s_\lambda = 6\alpha^2 S_\lambda$ of the above three orbits can be parametrized as

$$\begin{aligned} s_A(e) &= 2\pi(e + 0.0821e^2 + 0.0585e^6) && (0 \le e \le 1), \\ s_B(e) &= 2\pi(e + 0.0698e^2 - 0.0046e^4) && (0 \le e \le 2), \\ s_C(e) &= 2\pi(e - 0.0234e^2 + 0.0011e^4) && (0 \le e \le 2). \end{aligned} \tag{7}$$

We see from Eq. (7) that the periods $T_\lambda = dS_\lambda/dE$ for orbits A and B are slightly higher than 1 and that for orbit C is slightly below 1 (in units of T_0), exactly as we recognize it from the peak positions in Fig. 4. Note that due to their non-analytic energy dependence, these periods cannot be resolved exactly in the Fourier spectrum; in sampling an energy region $0 \le E \le 80$ for $\alpha = 0.04$ (corresponding to $0 \le e \lesssim 0.8$) for doing the Fourier transform, we obtain only their average values.

If we calculate the amplitudes $\mathcal{A}_\lambda$ in the Gutzwiller trace formula from the stability matrices of the three orbits numerically, we find that these have, indeed, approximately the ratios of the heights of the three peaks in the Fourier spectrum, if the amplitude of orbit C is multiplied by a factor 2 that corresponds to the two time orientations of the orbit. (Since orbits A and B are librations, they do not have this time reversal degeneracy.) One problem arises with the Gutzwiller amplitudes in the harmonic oscillator limit $E \to 0$ in which the classical orbits become degenerate, so that the amplitudes $\mathcal{A}_\lambda$ actually diverge. We remedy this situation by splining them for small E with their analytical behaviour $2E/(\hbar\omega)^2$ known for the harmonic oscillator result in Eq. (4) (see Refs. 19,20 for the details).

We now write down the semiclassical approximation of the level density, just keeping the lowest harmonics ($k = 1$) in the Gutzwiller trace formula (3):

$$\delta g_{cl}(E) = 3\left[\mathcal{A}_A \cos\left(S_A - \sigma_A\frac{\pi}{2}\right) + \mathcal{A}_B \cos\left(S_B - \sigma_B\frac{\pi}{2}\right) + 2\mathcal{A}_C \cos\left(S_C - \sigma_C\frac{\pi}{2}\right)\right]. \tag{8}$$

The overall factor 3 accounts for the symmetry of the HH potential. Strictly speaking, this factor should only be given to the amplitudes of orbits A and B, which occur in three distinct versions each. However, the amplitudes of the Fourier peaks just discussed favour the inclusion of this symmetry degeneracy factor also for orbit C. The Maslov indices σ_λ in Eq. (8) were found to be 5, 4 and 3 for orbit A, B and C, respectively.[20]

The final result of this semiclassical calculation is shown in the bottom row of Fig. 5. Note that the beats are almost exactly reproduced. When the symmetry factor 3 is not included for orbit C, the agreement becomes worse in that the beat minima are filled up due to an insufficient destructive interference between orbit C and the other two orbits. The reason for this apparent failure in the standard counting of the orbits is not yet understood and the object of further research.

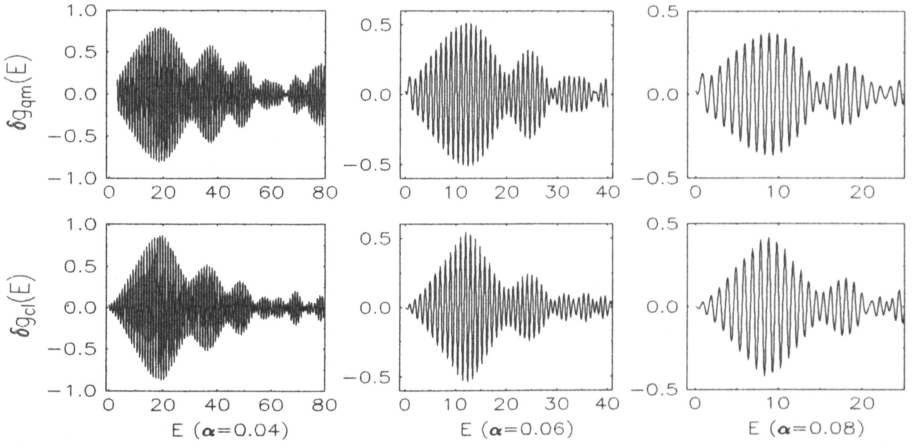

Fig. 5: Oscillating part of level density of Hénon-Heiles potential for three values of α *Upper part:* quantum-mechanical, *Lower part:* semiclassical results.

Apart from this counting problem, we have demonstrated that the periodic orbit theory is a useful tool for the semiclassical interpretation of the gross shell structure also in a classically chaotic system.

4. Acknowledgement

The work presented in this talk is the result of common projects with O. Genzken at Regensburg University (Sect. 2), and with R. K. Bhaduri at McMaster University, Hamilton, J. Law at Guelph University, M. V. N. Murthy at the Institute of Mathematical Sciences, Madras, and Ch. Maier at Regensburg University (Sect. 3). I am grateful to all these colleagues for the very stimulating and fruitful collaboration.

5. References

1. R. K. Bhaduri and C. K. Ross, Phys. Rev. Lett. **27**, 606 (1971); B. K. Jennings, Ann. Phys. (NY) **84** (1974) 1.

2. V. M. Strutinsky, Yad. Fiz. **3**, 614 (1966); Nucl. Phys. **A 95** (1967) 420; *ibid.*, **A 122** (1968) 1.

3. M. Brack and H. C. Pauli, Nucl. Phys. **A 207** (1973) 401; B. K. Jennings, Nucl. Phys. **A 207** (1973) 538; B. K. Jennings, R. K. Bhaduri and M. Brack, Nucl. Phys. **A 253** (1975) 29.

4. M. C. Gutzwiller, J. Math. Phys. **12** (1971) 343, and earlier references quoted therein.

5. R. Balian and C. Bloch, Ann. Phys. (NY) **69** (1972) 76, and earlier references quoted therein.

6. R. K. Bhaduri and B. K. Jennings (1974, unpublished).

7. M. Brack, Lecture notes (Regensburg University, 1993, unpublished).

8. M. C. Gutzwiller: *Chaos in Classical and Quantum Mechanics* (Springer-Verlag, New York, 1990).

9. *Chaos Focus Issue on Periodic Orbit Theory*, Chaos **2** (1) (1992).

10. V. M. Strutinsky, Nukleonika (Poland) **20** (1975) 679; V. M. Strutinsky and A. G. Magner, Sov. J. Part. Nucl. **7** (1976) 138; V. M. Strutinsky, A. G. Magner, S. R. Ofengenden, and T. Døssing, Z. Phys. **A 283** (1977) 269.

11. see, e.g., W. A. de Heer, Rev. Mod. Phys. **65** (1993) 611.

12. W. Ekardt, Phys. Rev. Lett. **52** (1984) 1925.

13. W. D. Knight, K. Clemenger, W. A. de Heer, W. A. Saunders, M. Y. Chou, and M. L. Cohen, Phys. Rev. Lett. **52** (1984) 2141.

14. H. Nishioka, K. Hansen and B. R. Mottelson, Phys. Rev. **B 42** (1990) 9377.

15. J. Pedersen, S. Bjørnholm, J. Borggreen, K. Hansen, T. P. Martin and H. D. Rasmussen, Nature **353** (1991) 733.

16. M. Brack, Rev. Mod. Phys. **65** (1993) 677.

17. O. Genzken and M. Brack, Phys. Rev. Lett. **67** (1991) 3286.

18. M. Hénon and C. Heiles, Astr. J. **69** (1964) 73.

19. M. Brack, R. K. Bhaduri, J. Law and M. V. N. Murthy, Phys. Rev. Lett. **70** (1993) 568.

20. M. Brack, R. K. Bhaduri, J. Law, Ch. Maier and M. V. N. Murthy, Phys. Rev. E (submitted); Regensburg University Preprint TPR-93-31 (1993).

21. K. T. R. Davies, T.E. Huston, and M. Baranger, Chaos **2** (1992) 215.